

W-AM-1S LATERAL DIFFUSION IN LIPID BILAYER MEMBRANES. W. W. Webb, School of Applied and Engineering Physics, Cornell University, Ithaca, New York 14853

Although the fluidity of lipid bilayer membranes and their sensitivity to phase transitions is well established by sensitive probes of molecular rotation times and by ion carrier permeabilities, direct measurements of lateral transport are scarce. We¹ have applied fluorescence correlation spectroscopy (FCS)² and fluorescence photobleaching recovery methods to measure the lateral diffusion coefficients of lipophilic fluorophore molecules that mimic phospholipids. Some of our observations of the dependence of lateral diffusion coefficients on lipid composition, temperature, retained solvent in black lipid membranes and the occurrence of phase transitions contrast with rotation and diffusion rates. The unique properties of diffusive transport in two dimensions and some implications of the two dimensional Stokes-Einstein paradox will be discussed. Our methods^{3,4} and results will be summarized and some implications for understanding transport processes in cell membranes discussed.

¹Participants include P.F. Fahey, D.E. Koppel, L.S. Barak, D.E. Wolf, E.L. Elson and D. Axelrod.

²D. Magde, E. Elson and W.W. Webb, Phys. Rev. Lett. 29, 705 (1972); E.L. Elson and D. Magde, Biopolymers 13, 1 (1974); D. Magde, E.L. Elson and W.W. Webb, Biopolymers 13, 29 (1974); E.L. Elson and W.W. Webb, Ann. Rev. Biophys. Bioeng. 4, 311 (1975).

³See poster presentation "Dynamics of Fluorescence Marker Concentration as a Probe of Mobility" by D.E. Koppel, D. Axelrod, J. Schlessinger, E.L. Elson and W.W. Webb.

⁴See poster presentation "Mobility Measurements by Analysis of Fluorescence Photobleaching Recovery Kinetics" by D. Axelrod, D.E. Koppel, J. Schlessinger, E.L. Elson and W.W. Webb.

W-AM-2S MEMBRANE STUDIES: POLYENE FLUORESCENT PROBES AND STATISTICAL MECHANICAL MODELS. Bruce S. Hudson, Department of Chemistry, Stanford University, Stanford, CA 94305

The use of the conjugated polyene fatty acid parinaric acid as a fluorescent probe of membrane structure has recently been reported [Sklar, *et al.*, Proc. Nat. Acad. Sci. USA 72, 1649 (1975); J. Supramol. Struct. (in press)]. Two geometrical isomers of this tetraene (*cis*, *trans*, *trans*, *cis* and *all trans*) and phosphatidyl cholines labeled with one conjugated chain have been prepared. This probe is biosynthetically incorporated by *E. coli* fatty acid auxotrophs. A sharp decrease in fluorescence intensity is observed at the phase transition of lecithin dispersions. Polarization and lifetime experiments will be discussed which demonstrate that this molecule is ideally suited for the measurement of rotational mobility. Partitioning experiments demonstrate the preference of the *trans* probe for solid phase regions of membranes. Parinaric acid is also a useful probe of lipid protein interactions because it quenches tryptophan fluorescence and shows a very strong induced CD on binding to proteins. The synthesis and uses of other polyene probes will also be discussed. A simple statistical mechanical model for the chain melting phase transition of lipid dispersions has been developed [Jacobs *et al.*, Proc. Nat. Acad. Sci. USA (in press, October, 1975)]. The translational motion of the choline molecule in two dimensions is treated as hard disks for which the partition function is known. The introduction of a *gauche* bond results in an area increase which is resisted by an average lateral pressure derived from the hard disk partition function. A mean field attractive van der Waals interaction stabilizes the system. This model is surprisingly accurate in its predictions of phase transition temperatures and enthalpies. Recent improvements in the treatment of the chain statistics and the calculation of phase diagrams will be discussed.

W-AM-3S THREE-DIMENSIONAL STRUCTURE OF PURPLE MEMBRANE. Richard Henderson and Nigel Unwin, MRC Laboratory of Molecular Biology, Hills Road, Cambridge, England.

The purple membrane has been extensively characterised by Stoeckenius and his colleagues. They have shown (a) that it is a specialised part of the cell membrane of *Halobacterium halobium* which functions in vivo as a light-driven proton pump, (b) that it is composed of identical protein molecules with a molecular weight of 26,000, linked covalently to the chromophore, retinal in a 1:1 ratio, and (c) that, together with lipid, the whole structure forms an extremely regular two-dimensional array (a crystal of space group P3). We have obtained a 7 Å resolution map of the purple membrane by electron microscopy of tilted, unstained specimens. The method we have used combines information from electron diffraction patterns and low dose electron micrographs. To obtain three-dimensional data, a number of diffraction patterns and micrographs were required with the specimen tilted at angles of up to 60° to the incident electron beam. The resulting map shows the distribution of scattering matter within the membrane at a resolution of 7 Å. The map contains numerous rod-shaped features aligned perpendicular to the plane of the membrane. There are seven rods in each asymmetric unit of the crystal, packed 10-12 Å apart. Since the X-ray pattern shows strong axial reflections at 1.5 Å and 5 Å, characteristic of the α-helix, we identify the seven rod-shaped features as α-helices which extend roughly perpendicular to the membrane for most of its 45 Å width. These α-helices account for 70-80% of the approximately 250 amino acid residues in a single protein molecule. The remainder of the polypeptide which cannot be discerned at this resolution presumably forms the regions of chain which join the α-helices together. Lipid bilayer regions fill the spaces between the protein molecules.

W-AM-4S THE STRUCTURE OF THE GRAMICIDIN A TRANSMEMBRANE CHANNEL. W. Veatch, Department of Molecular Biophysics and Biochemistry, Yale University, New Haven, Conn. 06520.

Gramicidin A is a linear polypeptide antibiotic that facilitates the passive diffusion of monovalent cations through lipid bilayer membranes by forming channels. I have prepared a series of derivatives of gramicidin C which are fully active analogs of gramicidin A and have desirable chromophoric properties. I will describe the results of three different experimental approaches which prove that the ion-conducting channel is a gramicidin dimer in equilibrium on the membrane with nonconducting gramicidin monomers. First, simultaneous conductance and fluorescence measurements were carried out on planar lipid bilayer membranes of varying thickness containing O-dansyl-tyrosine gramicidin C (Veatch, Mathies, Eisenberg, and Stryer, *J. Mol. Biol.* (1975)) in press). These experiments proved that the ion-conducting channel is a dimer of the nonconducting species, but they did not exclude the possibility that the channel is a tetramer and the nonconducting species a dimer. The second experiment took advantage of the fact that the single-channel conductance of O-(p-phenylazobenzene-sulfonyl)-tyrosine gramicidin C is 0.68 that of gramicidin A. In mixtures of the two gramicidins, a hybrid channel appears in addition to the two pure channels. The frequency of the hybrid is equal to $2ab$, where a^2 and b^2 are the frequencies of the pure peaks, strongly suggesting that the hybrid channel is a dimer. The third experiment uses fluorescence energy transfer to ascertain the mole fraction of these hybrid channels in phosphatidyl choline vesicles. O-(diethylaminophenylazobenzene-sulfonyl)-tyrosine gramicidin C quenches O-dansyl-tyrosine gramicidin C fluorescence with an R_0' of 30 Å. The dependence of the fluorescence on the quencher mole fraction excludes the possibility of a tetramer channel and shows that the efficiency of energy transfer within the dimer is 80-90%.

W-POS-A1 HYDROSTATIC PRESSURE EFFECT ON WATER FLOW IN FROG SKIN.

R.H. Parsons, P.L. Alberto† S.A. Sullman* and E.J. Schrenier† Biology Department, Rensselaer Polytechnic Institute, Troy, New York. 12181

Osmotic and hydrostatic water flow was measured using leg skin bags. Skin bags from each frog were paired, one serving as a control (osmotic gradient only) and the second as an experimental bag (osmotic and hydrostatic gradient). In bags with the epithelial surface facing outwards, 5cm H₂O pressure on the inside of the bag (corium) had no effect on the water flow. (Rates in mg·cm⁻²·hr⁻¹·200mOsm⁻¹ were 2.96±0.13(16) control and 2.75±0.22(16) experimental). When the orientation of the bag was reversed, a 5cm H₂O pressure inside the bag (epithelium) significantly increased the water movement. (Rates in mg·cm⁻²·hr⁻¹·200mOsm⁻¹ were 2.46±0.24(17) control and 3.88±0.32(17) experimental). This difference of 1.42±0.36(17) mg·cm⁻²·hr⁻¹·5cm H₂O⁻¹ represents a hydrostatic permeability expressed in units of osmotic permeability of 1380 mg·cm⁻²·hr⁻¹·200mOsm⁻¹. A 5cm H₂O pressure did not effect salt-linked water flow and the sucrose permeability in cm·sec⁻¹ with equal volume flow was 0.52±0.24(11) for control and 1.31±0.59(11) for experimental bags. Inulin space as % tissue water, with equal volume flow was 59.8±2.2(10)% for control and 56.6±2.3(10)% for experimental bags. With unequal volume flow the inulin space on the corium side was 44.4±5.1(10)% for control and 38.8±4.6(10)% for experimental bags. Sucrose space with unequal volume flow was 38.5±3.3(7)% for control and 35.5±3.8(7)% for experimental bags.

W-POS-A2 INTACT FROG SKIN EPIDERMIS RETAINS POTASSIUM BETTER THAN ISOLATED CELLS.

D. P. Valenzano and T. Hoshiko, Physiology Department, Case Western Reserve University, Cleveland, Ohio 44106

As previously shown (Fed. Proc. 33:216), isolated epidermis of *R. pipiens* can be depleted of its normal complement of potassium by 16 hours incubation in potassium-free half-strength Ringer's at 5C. Subsequent incubation at 22C for four hours in similar solutions containing as little as 1 mM/L potassium allows a significant reaccumulation of tissue potassium ($P < .0005$, $n = 124$). Despite the presence of potassium in the reaccumulation medium, the addition of 10⁻⁴ M ouabain leads to a further significant loss of tissue potassium. This may be contrasted to the effect of continued depletion in potassium-free media, wherein no further loss of tissue potassium occurs. These results lead us to believe that either ouabain induces a leak in the cell membrane, or that potassium in the extracellular space may be reaccumulated by skin cells in the absence of ouabain before it can diffuse out of that space. To distinguish between these possibilities experiments were performed on isolated cells of the skin. Cells were isolated by a modification of the method of Sayers, *et al.*, 1971 (Endo. 88:1063). It was found that cells prepared after depletion in potassium-free medium, lost potassium to a final level approximating that in the ouabain-treated intact epidermis. The viability of these cells was demonstrated by the fact that they were able to reaccumulate a significant quantity of potassium ($P < .01$, $n = 6$). Continued incubation of cells in either potassium-free, or 1 mM potassium with ouabain, showed no significant additional loss of potassium. We conclude that the extracellular space can retain potassium to a sufficient degree to allow it to be reaccumulated by cells of the intact epidermis. Supported by USPHS Grant No. AM-05865 (TH).

W-POS-A3 ³H-OUABAIN BINDING TO SPLIT FROG SKIN: THE ROLE OF THE Na-K ATPASE IN THE GENERATION OF SHORT CIRCUIT CURRENT. Peter M. Cala,* and Lazaro J. Mandel, Dept. of Physiology and Pharmacology, Duke University Medical Center, Durham, North Carolina 27710.

In epithelia, a direct involvement of the Na-K ATPase in active Na transepithelial transport has been postulated (Koeuf-Johnsen and Ussing, *Acta Physiol. Scand.* 42:298, 1958); however, no direct relationship has been demonstrated experimentally. The present study is an attempt to determine the role of the Na-K ATPase in active transepithelial Na transport by the frog skin. Preparations of bullfrog skin free of connective tissue were obtained by treatment with collagenase. Measurements of ³H-ouabain binding from the serosa] side were performed as a function of time in double label experiments utilizing ¹⁴C-mannitol as a marker for extracellular space. The ¹⁴C-mannitol space achieved saturation in approximately 30 minutes. Inhibition of active Na transport (short circuit current) was complete after 60-90 minutes in 10⁻⁶M ouabain, and after 45-70 minutes in 5 x 10⁻⁶M ouabain. Estimates of the number of Na-K ATPase sites were obtained from the number of ouabain molecules bound when complete inhibition was achieved, these values were: 1.2 ± 0.09 x 10¹² with 10⁻⁶M ouabain and 2.2 ± 0.44 x 10¹² molecules/mg dry weight with 5 x 10⁻⁶M ouabain. These values are very similar to those obtained in other cells. Furthermore, calculations based upon frog skin ATPase determinations (Kawada, *et al.*, *Comp. Biochem. Physiol.* 50:297, 1975) yield a value of 2.2 x 10¹² sites/mg dry weight. A rough correlation was found between the number of ³H-ouabain molecules bound and the percent inhibition of active transport. These preliminary data suggest that the Na-K ATPase is directly involved in active transepithelial Na transport in frog skin. (Supported by USPHS Grants AM-16024 and an NIH Postdoctoral Fellowship HL-01672).

W-POS-A4 THE USE OF MICROELECTRODE POTENTIAL AND RESISTANCE PROFILES TO ESTABLISH THE LOCATION OF THE K PUMP OF THE MIDGUT OF SILKMOTH LARVAE. J. T. Blankemeyer*, (Intr. by A. Kleinzeller) Department of Biology, Temple University, Philadelphia, Pa. 19122

The midgut epithelium of the fifth instar larva of *Hyalophora cecropia* (L.) is single layered and is essentially composed of two cell types, goblet and columnar. K is actively transported from hemolymph (basal) to lumen (apical). The K transport is associated with a very electrogenic transepithelial PD which is insensitive to ouabain and rapidly reduced by short periods of anoxia. Impalement of the epithelium with conventional microelectrodes produces two characteristic PD profiles. One profile, (HPD), has a typical basal PD of -25 mv. (referenced to the basal solution) and has high basal and apical membrane resistances. These resistances do not change when the K transport rate is varied. The second profile, (LPD), has a typical basal PD of -5 mv. and basal and apical resistances lower than HPD profiles. However the apical resistance of the LPD profile is inversely related to the K transport rate. The LPD and HPD profiles have been histologically identified with goblet and columnar cells, respectively, by intracellular injection of dye. A previous paper (Wood et al., J. Exp. Biol., 50, 169-178, 1969) had suggested an apical location for the K pump based on the sensitivity to anoxia of an apical step of the microelectrode potential profile. An ultrastructural study of the midgut (Anderson and Harvey, J. Cell Biol., 31, 107-134, 1966) suggested the goblet cell as the site of the K pump based on the apical location of the mitochondria in the goblet cells. This suggestion has been confirmed by the profile evidence in this paper which associates the K pump with LPD profiles and associates LPD profiles with goblet cells.

W-POS-A5 CARBONIC ANHYDRASE: AN EPITHELIAL ENZYME DIFFERENTIALLY MODULATED BY cAMP. M. M. Cassidy, S. P. Bartels*, and M. F. Armaly*, Departments of Physiology and Ophthalmology, George Washington University Medical Center, Washington, DC 20037.

Carbonic anhydrase (CAH) is an enzyme anomalously associated with the translocation or elaboration of specific body fluids in most epithelia. Because of recent ancillary transport studies linking fluid formation to cyclic AMP we have studied the effect of cAMP on tissue carbonic anhydrase activity in bovine iris-ciliary process, rabbit gastric mucosa and cat colonic epithelium. The assay used is a microtechnique which determines the rate of CO_2 driven proton release in a system in which the ΔpH occurring during the 2 sec assay period is less than 0.1 pH unit. Calibration with purified bovine CAH yields a slope of 2.26 ± 0.03 pmoles $[\text{H}^+]/\text{sec}/\mu\text{g}$ of pure enzyme and complete inhibition of proton production in the presence of acetazolamide (10^{-4} M). Microdissected and homogenized samples of the epithelia were incubated for periods of 20 min to 2 hrs in 3 mM ATP, 10 mM Mg_2Cl , 2 mM theophylline and dibutyl cyclic AMP. Paired incubation fluids lacked DB cAMP. Control values for CAH activity/mg protein were: colon mucosa 17.5 pmoles/sec, gastric mucosa 3.52 pmoles/sec and iris-ciliary process 9.38 pmoles/sec. Incubation with 2 mM DB cAMP inhibited colonic activity by 90% ($P < 0.01$), iris-ciliary activity by 43% ($P < 0.01$) and stimulated gastric mucosal activity by 30% ($P < 0.02$). Modulation of CAH activity in homogenates was ATP, Mg^{++} , time and temperature dependent and 5' AMP was without effect. The differential response of this enzyme in these tissues to enhanced cAMP levels could partially explain such diverse observations as the reduction in ocular pressure by adrenergic agonists and the reversal of normal fluid absorption in the colon by bile salts and cholera toxin.

W-POS-A6 THE PENETRATION OF UREA IN THE TOAD URINARY BLADDER: THE EFFECT OF ADH. M. Parisi and O.A. Candia, Department of Biophysics, Fac of Medicine University of Buenos Aires, Argentina, and Dept. of Ophthalmology, Mount Sinai Medical Center, New York, N.Y., 10029.

It has been recently postulated that urea and water move across different biological membranes through independent pathways. This is supported by the dissociation between water and urea movements induced by different agents. We have now studied the uptake of urea C^{14} into everted bladder sacs comparing this uptake with the appearance, over short time periods (up to 2 min) of urea C^{14} into the serosal fluid. The obtained values for K_{trans} , either at rest or under ADH were similar in both cases and similar to those previously reported for steady-state condition (28 ± 8 and 432 ± 25 $\text{cm} \cdot \text{sec}^{-1} \times 10^{-7}$ respectively). No accumulation of urea C^{14} inside the tissue was detected indicating that the mucosal border is the limiting step for urea movement in all cases. Comparative studies of urea and inuline uptake from the serosal side showed that urea equilibrated with all the water cell in less than 30 sec. Finally the kinetics of increase in urea permeability induced by ADH was similar to the kinetics of increase in water flux ($T_{1/2}$ 5.2 ± 0.3 and 5.8 ± 0.4 min respect) Serosal hypertonicity also increases water and urea permeabilities and a strong parallelism between both responses was again observed (Both developed after a latency period of 25 min.). These results suggest that the mechanisms regulating urea and water permeability must be at least partially linked, even that the final step could be different.

W-POS-A7 VALIDATION IN TOAD BLADDER OF A GENERAL SEMI-EMPIRICAL FORMULATION FOR PASSIVE TRANSMEMBRANE ION FLUXES ACROSS ELECTRICAL AND CHEMICAL GRADIENTS. J. S. Chen* and M. Walser, Depts. of Pharmacology and Medicine, Johns Hopkins University School of Medicine Baltimore, Md. 21205.

We have previously reported (J. Memb. Biol. 18:365, 1974; 21:87, 1975) that, in the absence of concentration gradients, bidirectional sodium fluxes through both active and passive paths in toad bladder during voltage clamping follow a modified flux ratio equation, $\ln(\bar{J}/J) = Q(zF/RT)(\psi - E)$, where E is the potential at which $J = \bar{J}$, and Q is the ratio of bulk ion diffusion coefficient, D (or permeability, P) to tracer diffusion coefficient, D^* (or permeability, P^*). $Q_{Na} < 1$ for passive flux, $Q_{Na} > 1$ for active flux, for reasons unknown. By extension to chemical gradients at zero potential, $\ln(\bar{J}^0/J^0) = (Q/2)\ln(C_1/C_2) + \ln zFJ$. These relationships also yield expressions for P and P^* as functions of C_1 , C_2 , and Q . The empirical assumption underlying these equations is that Q is invariant. Bidirectional sodium fluxes across toad bladder sacs poisoned with ouabain (1.89×10^{-3} M) were measured with serosal $[Na]$ fixed at 114 mM and mucosal $[Na]$ (C_M) = 3, 12, 40, or 114 mM. Potential, ψ , was clamped to 0 mV, 100 mV, or the Nernst potential. Close agreement was found between experimental and theoretical dependence of \bar{J} , J , \bar{J}/J , P and P^* on C_M and on ψ . Q remained nearly constant (0.50-0.57) throughout this wide range of chemical and electrical gradients. "Isotope interaction" cannot account for these results since Q expresses a membrane property of major importance in determining bulk flow of solute even when isotopes are absent. An adequate explanation of, or name for, this interesting membrane property is as yet lacking.

W-POS-A8 H^+ AND HCO_3^- ACCUMULATION IN FROG GASTRIC MUCOSA AS ESTIMATED FROM DMO WASHOUT KINETIC. Leopoldo Villegas, Centro de Biofísica y Bioquímica, Instituto Venezolano de Investigaciones Científicas, IVIC, Caracas 101, Venezuela.

Experiments were done to quantify the effects of the H^+ and HCO_3^- accumulation on the pH of the extracellular compartments. The experiments are based on the assumption that the DMO (5,5-dimethylloxazolidine-2,4-dione) diffuses into and out of the extracellular compartments in both the A^- and the AH forms, while the diffusion into and out of the cellular compartment occurs, mainly in the AH form. The washout of mucosae incubated during 90 min in solution with 10^{-4} M C-14 DMO can be fitted to an exponential curve with 3 phases of time constants: the 1st between 0.26 and 0.38 min $^{-1}$; the 2nd between 0.084 and 0.096 min $^{-1}$; and the 3rd between 0.014 and 0.018 min $^{-1}$. The DMO activity recovered in the 1st phase corresponds to the H-3 inulin space measured in the same mucosae. The activities recovered in the 2nd and 3rd phases correspond to the DMO from the cellular compartment. These effluxes are functions of the cellular and extracellular AH activities. The AH form of the DMO in the restricted extracellular compartments is determined by the pH of these compartments and by the bathing solutions total DMO concentration. The ratios of the activities recovered in the serosal surface to those recovered in the mucosal surface were 6.03 ± 1.94 ; 4.45 ± 0.92 ; and 6.69 ± 1.36 when the bathing solutions' pH were: 6.9; 7.4; and 7.9, respectively. A model is proposed in which the effective pH of the extracellular serosal compartment is between 0.73 and 0.89 units higher than that of the extracellular mucosal compartment. This difference is independent of the bathing solutions' pH.

W-POS-A9 INTERACTIONS BETWEEN OSMOTICALLY INDUCED FLOW AND SOLUTE-COUPLED FLOW IN THE RAT ILEUM. M.L. Fidelman*, (Intr. by D. Hare), Dept. of Biophysical Sciences, SUNYAB; Buffalo, New York 14214

A comparison of the current models in the literature describing osmotically induced flow and solute-coupled flow suggests that these two flows are not independent. A pair of two-compartment membrane chambers is used simultaneously to obtain concurrent measurements of the net Na flow and the bulk fluid flow. The solute-coupled and/or osmotically induced flow is measured volumetrically in a constant bore capillary and Na^{22} is used to measure the net Na transport. A tissue preparation method has been developed which maintains tissue viability and stability for a 2-3 hour period and permits a series of both test and control experiments to be run on adjacent sections of the same ileum. The results show that when an osmotic gradient of 170 mOsm/L from mucosa to serosa (M \rightarrow S) is superimposed on solute-coupled flow, the resultant flow is greater than the sum of the separate flows. When the gradient is superimposed from S \rightarrow M, the resultant flow remains from M \rightarrow S and is greater than the solute-coupled flow when there is no osmotic gradient. The results show that osmotically induced flow and solute-coupled flow are not independent.

W-POS-A10 INFERENCES CONCERNING RENAL MEDULLARY FUNCTION FROM STUDIES USING THE CENTRAL CORE MODEL. D. M. Foster and J. A. Jacquez, Dept. of Physiology, The University of Michigan, Ann Arbor, Michigan 48104

The central core model is presented as a model of a concentrating engine the equations of which can be solved numerically and from which inferences concerning renal medullary function can be deduced. Initial studies show that using the geometric and thermodynamic parameters for rabbit kidney, a medullary concentration gradient, and urine flow rate and concentration are generated that fall within the range of those values obtained experimentally. The parameters and inputs are then varied in a series of input-output studies from which the inferences on medullary function are drawn. As an example, we found that with all other parameters being equal, there is an optimal flow rate into the descending limb of Henle (DHL) with respect to the generation of a medullary concentration gradient; values of inflow rates above or below this optimal flow rate result in a decreased gradient. This and the phenomenon of high flow rates in the vasa recta washing out the gradient suggest that one of the immediate mechanisms of controlling this gradient involves control of medullary blood flow and inflow into the DHL, and that these two are linked aspects of one mechanism, the control of the resistance of the efferent arterioles of the juxtamedullary glomeruli.

W-POS-A11 THE EFFECTS OF DIGITONIN ON SOME KINETIC PARAMETERS OF THE "PARTIAL REACTIONS" OF CANINE KIDNEY Na^+ , K^+ -ATP-ASE. Charles G. Winter, Department of Biochemistry, University of Arkansas College of Medicine, Little Rock, Arkansas 72201.

Using highly enriched preparations of Na^+ , K^+ -ATPase from dog kidney, the effects of digitonin on the Na^+ -dependent, ouabain-sensitive ADP-ATP exchange and K^+ -dependent, ouabain-sensitive phosphatase activities of the enzyme were studied. The preparations used showed 2 major bands on SDS-polyacrylamide gel electrophoresis and had specific activities of 1200-1500 $\mu\text{mol/mg/hr}$. In confirmation of previous findings with impure preparations, inhibition of greater than 95% of the Na^+ , K^+ -ATPase activity by digitonin resulted in no loss of ouabain-sensitive exchange, as well as survival of about 70% of the ouabain-sensitive acetyl phosphatase activity. Under the same conditions, however, only 20% of the K^+ -dependent, ouabain-sensitive p-nitrophenyl phosphatase activity remained. Investigation of the K^+ concentration-dependence of both phosphatase activities revealed that digitonin treatment caused a 4-fold increase in the apparent K_m for the acetyl phosphatase but a 7-8-fold rise in that for the p-nitrophenyl phosphatase. The value of the Hill coefficient remained close to 2 in both cases, indicating that "uncoupling" the two phosphatase activities from the ATPase activity did not alter the cooperativity among the several K^+ sites. Similar results were obtained for K^+ activation of the ouabain-sensitive ADP-ATP exchange activity. The $I_{0.5}$ value for ouabain inhibition of phosphatase activity was lowered considerably by digitonin, while that for inhibition of exchange was somewhat increased. Sensitivity of all the "partial reactions" to harmaline was also increased. These results indicate that digitonin treatment perturbs Na^+ , K^+ -ATPase structure to an extent sufficient to affect several cation regulatory and inhibitor sites. Supported in part by NIH grant AM-16483.

W-POS-A12 FURTHER CHARACTERIZATION OF THE Na -STIMULATED, OUABAIN INSENSITIVE ATPase FROM GUINEA-PIG KIDNEY CORTEX. F. Proverbio, M. Condrescu-Guidi*, M. Pérez-González† and G. Whittembury, Instituto Venezolano de Investigaciones Científicas (IVIC), Caracas, Venezuela.

We have described a K-independent, Ouabain insensitive Na-extrusion in guinea-pig kidney cortex slices. If the $(\text{Na}+\text{K})$ stimulated ATPase were the system providing the energy for this Na-extrusion, it would be expected that inhibition of this enzyme complex would inhibit it; since this is not so, the possibility was raised that other energy supplies could be involved in bulk Na transport in the kidney. Working with microsomal fractions of guinea-pig kidney cortex, we found an Mg-dependent ATPase activity which showed to be Na-stimulated, Ouabain insensitive and completely inhibited by 2 mM Ethacrynic Acid, or 0.1 mM Furosemide. This Na-stimulation is not present in fresh preparations but it becomes evident in aged fractions. This finding suggests either that we are in the presence of a different type of ATPase activity that is masked or inhibited in the fresh preparations, or that the Mg-dependent of $(\text{Na}+\text{K})$ -stimulated ATPase undergoes transformations to give an ATPase with new characteristics. The influence of the pH was studied on the system; it was found that the pH of the microsomal preparations was not stable but dropped with time, reaching values of 6.5 at about the same time the ATPase system shows the Na stimulation; which, on the other hand, does not appear if precautions are taken to avoid the pH drop. Even more, if the microsomal fraction is resuspended in a medium at a pH of 6.5 immediately after preparation, the appearance of the Na-stimulation is drastically fastened. The optimal pH of the ATPase Na-stimulated was found to be 6.8.

W-POS-A13 EFFECTS OF MUCOSAL SOLUTION HYPEROSMOLALITY ON THE CELLULAR AND SHUNT PATHWAYS OF NECTURUS GALLBLADDER (NGB) EPITHELIUM. L. Reuss and A.L. Finn, Department of Medicine, University of North Carolina School of Medicine, Chapel Hill, N.C. 27514.

The effects of hyperosmolar mucosal solutions on the cellular and shunt pathways of the epithelium of NGB were studied by measuring the electrical potentials across the tissue (V_m) and across the cell membranes (apical: V_{mc} ; basal-lateral: V_{cs}), along with the electrical resistances of the tissue (R_t), the cell membranes (R_a , R_b), and the shunt (R_s). Mean values before and after doubling the osmolality of the mucosal solution with sucrose (S) are shown in the table (V 's, mV; R 's, $\Omega \cdot \text{cm}^2$):

CONDITION	V_m	V_{mc}	V_{cs}	R_t	R_a	R_b	R_s
Ringer	3.2	56.2	59.4	450	3880	4900	480
Ringer + Sucrose	1.5	32.7	34.2	580	1810	4580	680
P	<.02	<.01	<.01	<.02	<.02	NS	<.05

When NaCl was added instead of S, R_t increased only transiently (<3 min) and then fell. In the steady-state, cellular effects were similar, but R_t and R_s were significantly decreased. The magnitude of the changes in V_{mc} and V_{cs} (as compared to V_m) indicate that, in addition to a shunt diffusion potential, mucosal hyperosmolality produces large changes in one or both cell membrane EMF's. The decrease in R_a is due to an increase in apical membrane Cl or Na conductance. The observation that S and NaCl effect opposite changes in R_s indicates that narrowing of the lateral intercellular spaces by the induced osmotic water flow is not the cause. The direction and time course of the changes in R_s may depend on the relative permeabilities of the luminal end of the limiting junction to water and the added solute. Supported by USPHS Grant #AM-17854

W-POS-A14 RELATION BETWEEN PERMEABILITY AND ULTRASTRUCTURE CHANGES INDUCED BY ANTIDIURETIC HORMONE. J. Chevalier*, J. Bourguet and J. S. Hugon*. Inst. de Pathol. Cell INSERM, U.48, Hôpital de Bicêtre; dept. de biol. CEN SACLAY, France and Dept. of Pathol., Medical Center, Univ. of Sherbrooke, P.Q. CANADA.

It has been shown recently that the luminal plasma membrane, which is the presumed limiting permeability barrier in frog urinary bladder has a typical freeze etch structure. The A face of this membrane exhibits a particularly low particle density, and presents during hydroosmotic challenge particle clusters which appear to be directly linked to permeability variations (see for instance J. CHEVALIER et al Cell Tiss. Res. 1974, 152, 129). We suggest here that transmembrane pathways are created by the junction of separate hemi-channels located in the outer and inner leaflets of the membrane, and somehow linked to the membrane associated particles. They could for instance be located in the hydrophilic core of the particle or result from dislocations of the hydrophobic lipid monolayer created by the presence of the particles. The low density of particles observed on the apical A face at rest would correspond to a low hemi-channel density of the inner leaflet. This would result in a low water permeability of the whole membrane despite a high hemi-channel density in the outer (B face). On the contrary, the presence of areas with a high hemi-channel density in the inner leaflet would make more probable a junction between outer and inner hemi-channels and result in a higher permeability. Ultrastructural alterations would thus interest mainly the inner leaflet directly accessible from the cytoplasm.

W-POS-A15 ANTHROYL-OUABAIN: A SPECIFIC FLUORESCENT PROBE FOR THE CARDIAC GLYCOSIDE BINDING SITE OF THE Na-K ATPase. P.A. George Fortes, Department of Biology, University of California, San Diego, La Jolla, California 92093

Anthroyl-ouabain (AO) was synthesized by esterification of an anthracene molecule to the rhamnose of ouabain. AO inhibition of Na-K ATPase was measured by incubating human RBC ghosts with various concentrations of AO (in the presence of ATP, Mg & Na) for 1 hr. at 37°C, washing, and assaying for the remaining Na-K ATPase activity. Under these conditions 50% inhibition was observed with 0.1 μM AO compared with 0.05 μM for ouabain. If no ATP is included in the preincubation no inhibition is observed with either ouabain or AO. Fluorescence spectra of AO depend strongly on the solvent. λ_{max} and relative intensities are, respectively: H₂O: 490 nm, 1; methanol: 465 nm, 14; ethanol: 463 nm, 24; butanol: 462 nm, 31. Excitation peaks in ethanol are: 255, 330, 345, 362 and 381 nm, and in H₂O: 255, 350, 365 and 385 nm. Albumin, detergent micelles and RBC ghosts have no effect on AO fluorescence. Purified Na-K ATPase (0.5 mg/ml) from rabbit kidney microsomes (Jørgensen, BBA 356:36 (1974)): a) enhances AO (0.5 μM) fluorescence about 100% in the presence of MgATP and Na, or Mg and inorganic phosphate; b) shifts λ_{max} from 490 to 470 nm; c) gives a new excitation peak at 280 nm, due to energy transfer from tryptophan that must be near the binding site. Preincubation with ouabain eliminates the fluorescence enhancement, the spectral shifts and the 280 nm excitation peak. Fluorescence titrations suggest that AO binding saturates around 0.5 μM AO at 37°C. These results indicate that AO is a sensitive fluorescent probe and highly specific for the cardiac glycoside binding site of the Na-K ATPase. Information on the fluorescence parameters of the bound AO and their changes with various ligands will be presented. (Supported by a grant-in-aid from the American Heart Association and USPHS grant RR-08135.)

W-POS-A16 STANDING GRADIENT OSMOTIC FLOW: EXAMINATION OF ITS VALIDITY USING AN ANALYTICAL METHOD. J.J. Lim and J. Fischberg, Depts. of Ophthalmology and Physiology, College of Physicians and Surgeons, Columbia University, New York, N. Y. 10032

The concentration and velocity profiles for solute as a function of distance along intercellular channels in epithelia under the assumptions involved in the "standing-gradient" hypothesis have commonly been obtained by numerical methods using suitable computer techniques because the differential equation governing those parameters is non-linear. Instead of using that procedure, we have obtained analytical solutions to that differential equation by the use of perturbation theory. The solutions thus obtained with a second order correction compare extremely well with the data published previously on concentration and velocity profiles and the osmolarity of the fluid transported for both the "backwards" and the "forwards" cases. The present approach is simpler, less time-consuming, and yields an amount of information analogous to that obtained with computer techniques. This method has further allowed us to examine the validity of the "standing-gradient" hypothesis for fluid transport in a particular case. That hypothesis has been presently scrutinized using parameters which were experimentally measured or estimated (diffusion constant, permeability, rate of transport, radius, length of the channel, and location of the pumping sites) for the "backwards" fluid transport system of the corneal endothelial layer. With the values presently used for these parameters, the near-isotonicity of the transported fluid (which separate observations suggest) could not be explained by the "standing-gradient" model, which yields instead a fluid between 3 to 100 times hypertonic. The concentration and velocity profiles obtained by numerical and by analytical methods will be presented and the validity of the "standing-gradient" osmotic theory will be discussed for the endothelial and similar preparations. (NIH Support).

W-POS-A17 SELF-CONSISTENT ANALYSIS OF ARTERIAL UPTAKE OF CHOLESTEROL FROM PERFUSING SERUM. M.H. Friedman, Applied Physics Laboratory, The Johns Hopkins University, Laurel, Md. 20810.

Caro's data (Cardiovasc. Res. 8: 194-203, 1974) on the shear-dependent in vitro uptake of ^{14}C -4-cholesterol from serum flowing through canine carotid arteries are interpreted using an apparently new equation relating interfacial concentration (C_w) and flux (g) under a steady concentration boundary layer. The concentration and flux are presumed to be related by $g = kC_w$, where k is (shear-dependent) arterial permeability. When the shear is uniform, the variation of C_w with distance from the origin of the test segment (X) is a function of a single parameter $\gamma = k^3 x / (D^2 S)$ (D =solute diffusion coefficient, S =wall shear rate), whose magnitude measures the relative resistances to transport in the fluid and at the interface. The largest γ in Caro's experiments is 3×10^{-7} , indicating that his tracer uptake data correctly measure interfacial permeability, and confirming his and Nerem's (Caro and Nerem, Circ. Res. 32: 187-205, 1973) conclusion that the major resistance to cholesterol uptake is at the wall. Caro's permeability data are used to predict the variation of cholesterol uptake along the wall of a branch modeling the aortic bifurcation. In the branch, the shear and hence the cholesterol permeability vary along the wall. The wall flux is calculated to follow k very closely; the shape of the flux profile depends essentially entirely on the fashion in which the permeability responds to shear. The resistance of the concentration boundary layer is again trivial, suggesting that hemodynamic factors act to produce local variations in lipid uptake in arterial segments predisposed to atherosclerosis through a corresponding variation in the shear-dependent permeability of the vascular wall. Supported in part by NIH Grant HL14207. I am grateful to L. W. Ehrlich for helpful discussions and essential calculations.

W-POS-B1 STRUCTURAL AND GENETIC RELATIONSHIPS AMONG HUMAN LIPOPROTEINS. W.C. Barker and M.O. Dayhoff, National Biomedical Research Foundation, Georgetown University Medical Ctr., 3900 Reservoir Road, NW, Washington, D.C. 20007

Computer examination of the amino acid sequences of human apolipoproteins reveals evidence of distant relatedness between proteins, of internal gene duplications, and of structural periodicities. Apolipoprotein Gln-1 (apoLP-Gln-1) has a prominent 11-residue periodicity throughout much of its structure. Several other apolipoproteins have fewer but longer periodicities; for example, apoLP-Gln-2 can be divided into three similar sections of 25-27 residues. Two others, apoLP-Ala and apoLP-Ser, share this apparent 27-residue duplication. Independent tests of sequence relatedness indicate that these three share a common genetic ancestor. Furthermore, apoLP-Ser appears to have an 11-residue periodicity within each half of its structure. Parts of apoLP-Ala and apoLP-Gln-2 also show this periodicity. A plausible evolutionary history that assumes that both the 11- and 27-residue periodicities are due to ancient gene duplications will be presented. The sequence regularities to be expected from such a genetic history will be compared with the proposed locations of amphipathic helices (those having a polar face opposite a hydrophobic face), which are presumed to be important in the binding of phospholipids to these proteins. *Supported by NIH Grant HD09547.*

W-POS-B2 IMPROVED COMPUTER METHODS TO DETECT DISTANT RELATIONSHIPS BETWEEN PROTEIN SEQUENCES. M.O. Dayhoff, R.M. Schwartz, W.C. Barker, and B.C. Orcutt*, National Biomedical Research Fndn., Georgetown Univ. Med. Ctr., 3900 Reservoir Road, NW, Washington, DC 20007

Almost all human proteins have evolved through the accumulation of small changes in sequence which will be traceable in detail back to the early vertebrates. Homologues of many proteins are also still recognizable in the other eukaryotes and bacteria through similarity in protein sequence. In a continuing effort to clarify the general evolutionary scheme from sequence information, we have recently improved the three main statistical computer methods in use. These methods all depend on accumulated contributions from the comparison of each amino acid in one sequence with the corresponding one in the other, as specified in an input matrix of amino acid pair scores. (1) The "alignment score" method determines the best alignment for two sequences. Two parameters may now be specified: one penalizes additional positions in the overall alignment and the other penalizes each cut made in either sequence. The score for the real sequences is compared with the (normal) distribution of scores from randomized sequences and the probability that the real score is a member of the random population is calculated. (2) In the "fragment comparison" method, fragments of a given length from one sequence are compared with all fragments of the same length from a second sequence (or from itself). The distribution of scores from real sequences is compared with those from randomized sequences. A sensitive new feature calculates, for every score, the statistical significance of the total number of scores above that score. (3) The "search score" method is based on a comparison of a short sequence with all fragments of equal length in a data collection. The distribution of high scores is examined. Examples of specific relationships detected with the three methods will be displayed. *Supported by NIH Grant GM-08710.*

W-POS-B3 VARIOUS CONFORMATIONAL STATES OF DNA IN CHROMATIN REVEALED BY ETHIDIUM BROMIDE BINDING STUDIES. J.J. Lawrence* Cancer Center of Hawaii, University of Hawaii, Honolulu, HI. 96822

The binding of Ethidium bromide to native chromatin, histone depleted chromatin by either sodium chloride or sodium deoxycholate and non-histone proteins depleted chromatin has been studied and quantitatively estimated after revision of the binding model used to describe the system. 95% of the DNA has been found to be accessible in native chromatin and the binding occurs on two types of high fluorescent binding sites. 13% of chromatin DNA has a binding constant 700 times higher than that of pure DNA. The remaining 82% have a binding constant consistent with the ionic strength effect expected from histone composition. Histone H₁ and tertiary structure of DNA generated by the octamer structure are both required to maintain this special binding process. Non-histone protein extraction increases slightly the number of higher affinity binding sites while covalent binding of proteins to DNA by formaldehyde reduces only the number of low affinity binding sites, but not that of high affinity. Structural and functional implications of these results will be discussed.

W-POS-B4 ALTERATION OF POLYNUCLEOTIDE SECONDARY STRUCTURE BY RIBOSOMAL PROTEIN S1.

D. G. Bear, R. Ng,* D. Van Derveer,* N. P. Johnson, G. Thomas,* T. Schleich, and H. F. Noller,* Division of Natural Sciences, University of California, Santa Cruz, CA 95064

Ribosomal 30S protein S1 causes disruption of the secondary structure of certain pyrimidine containing polynucleotides. Helical poly U, poly (C,U), and neutral and acidic poly C are stoichiometrically converted to their partially or completely thermally denatured forms, as revealed by circular dichroism. Of the several double and triple stranded helical polynucleotides tested that contain one polypurine strand and at least one polypyrimidine strand, only the DNA-RNA hybrid poly rA·poly dT is perturbed. In the presence of S1, this hybrid undergoes a transition to a new structure which has a circular dichroism spectrum unlike either the native or thermally denatured forms. Intercalated ethidium bromide is released from poly rA·poly dT by S1, confirming a loss of helicity. The translation inhibitor autintricarboxylic acid completely inhibits the action of S1 on polypyrimidines, but has no effect on the conformational perturbation of poly rA·poly dT. These observations may be related to the possible conformational changes in the 30S ribosomal subunit induced by protein S1. (Supported by USPHS grant 17129 (to H.F.N.) and NSF grant BMS 75-17114 (to T.S.).)

W-POS-B5 THERMAL TRANSITIONS IN VIRAL DNAs: QUANTITATION AND MAPPING. D. L. Vizard and A. T. Ansevin. The University of Texas System Cancer Center, M. D. Anderson Hospital and Tumor Institute, Houston, Texas 77025.

High resolution thermal profiles of viral DNAs display a number of thermal subcomponents (thermalites) which are believed to reflect the heterogeneity among different local regions along the length of the genomes. The length of cooperatively melting base sequences, as determined from the area of thermalites in first derivative denaturation profiles, is in the range of gene-sized segment of DNA. For several viral DNAs a correlation can be made between the total number of thermalites and the number of identified genetic units, and in some instances between thermalite sizes and expected sequence sizes of the genes. However, it is not clear whether the discrete nature of DNA thermal denaturation is related to genetic factors or is simply a reflection of the fluctuations of thermal stability expected from quasi-randomly distributed base pairs.

The positions of sequences giving rise to thermalites can be mapped with the aid of several techniques, such as selective digestion of terminal sequences by exonuclease, isolation of restriction endonuclease fragments, and deductions from hysteresis renaturation patterns for partially melted DNAs. Attempts to compare thermalites with the published denaturation sites of DNAs mapped by electron microscopic techniques demonstrates that little numerical correlation exists; the number of significant thermalites consistently exceeds the number of microscopically mapped denaturation sites. This discrepancy probably arises because of the non-equilibrium nature of the microscopic mapping method.

W-POS-B6 SEQUENCE PREFERENCES IN THE INTERCALATIVE BINDING OF ACTINOMYCIN D AND ETHIDIUM BROMIDE TO NUCLEIC ACIDS. T.R. Krugh, Y.-C. Chen,* and C.G. Reinhardt, Department of Chemistry, University of Rochester, Rochester, New York 14627.

Spectroscopic (NMR, visible, fluorescence, and circular dichroism) studies of actinomycin D complexes with deoxydinucleotides and with DNA have shown that actinomycin D binds stronger to guanine-pyrimidine sequences than to the other sequences available as intercalation sites. Ethidium bromide complexes with both deoxydinucleotides and ribodinucleoside monophosphates, as well as DNA, have shown that ethidium bromide prefers a pyrimidine-purine sequence when compared to the purine-pyrimidine sequence. The source of these sequence preferences is most likely a result of "stacking" forces. The use of model compounds for studying drug-nucleic acid complexes and the general implications of these results will be discussed.

W-POS-B7 PMR STUDIES ON THE NH-N HYDROGEN-BONDED AND METHYL, METHYLENE PROTON RESONANCES OF tRNA^{phe} AND phe-tRNA^{phe}. L.S.Kan, P.O.P.Ts'o, M.Sprinzel*, F.v.d.Haar*, and F.Cramer*, Johns Hopkins U., Baltimore, Md. 21205 and Max Planck Institute, Göttingen, W. Germany.

The NH-N hydrogen bonded proton resonances of yeast tRNA^{phe} and phe-tRNA^{phe} (tRNA^{phe} covalently linked with a phenylalanine by an amide bond to 3'-NH₂ position of modified A₇₆) were compared at 250 MHz, 27°C in H₂O, 0.01 M MgCl₂, 0.2 M NaCl, 0.002 M EDTA, and 0.01 M PO₄ buffer, pH 6.5. At least one signal around -13 ppm (E peak, JMB, 78, 71 (1973)) and perhaps one proton in the peak at -13.7 ppm (B peak) disappeared in the phe-tRNA^{phe}. Candidates for the E peak are GC₁₁, AU₂₉, 50, Aψ₃₁ (JMB, 78, 71 (1973)); G₁₉C₅₆, T₅₄-m¹A₅₈ (tertiary base pairs, Nature, 257, 287 (1975)). Candidates for the B peak are AU₁₂, 52. Data clearly indicate a difference in conformation between tRNA^{phe} and phe-tRNA^{phe}. The methyl and methylene resonances of tRNA^{phe} were also studied in D₂O with 0.01 M MgCl₂ at 220 and 360 MHz from 40-98°C. Three major differences were found in comparison with tRNA^{phe} without Mg⁺⁺ (BBRC, 59, 22 (1974)): (1) The native-coil transition occurs within a very narrow temp. range. (2) The rT base exists in two different conformations in the native form. The rT resonances were observed in two peaks (1, ~1.5 ppm) at low temp., confirming the report on E. coli tRNA^{val} (Biochemistry, 14, 3612 (1975)). This splitting phenomenon of the rT resonance was also observed in the fragment of 47-76 in Mg⁺⁺ (1.3, 1.7 ppm at 48°C). (3) The signals from m²G₁₀, P₁₆, 17, m²G₂₆, m³C₄₀, 49, m⁷G₄₆, rT₅₄, and m¹A₅₈ are sharp at high temp. broadened at the transition temp. and sharp again at low temp. except m²G, indicating their involvement in the native form. The methyl resonances from the anticodon loop are not affected by Mg⁺⁺. No difference in the methyl and methylene resonances of tRNA^{phe}, tRNA^{phe}, and phe-tRNA^{phe} from 40-90°C was found in the absence of Mg⁺⁺. (Supported by NIH and NSF)

W-POS-B8 CONFORMATIONAL ANALYSIS OF NUCLEIC ACIDS USING CARBON-13 NMR HETERONUCLEAR COUPLING CONSTANTS. J. L. Alderfer and P. O. P. Ts'o, Division of Biophysics, School of Hygiene and Public Health, The Johns Hopkins University, Baltimore, Md. 21205

Several dihedral angles (C-N, χ ; C3'-O3', ω ; C5'-O5', ϕ) which are important in determining nucleic acid structure can be obtained by ¹³C-NMR. Proton-coupled spectra of uridine, 3'-UMP, 5'-UMP, 3'-CMP, and 5'-CMP in aqueous solution (0.5M, pH 8.4, 30°) produce two coupling constants (³J_{C2',H1'} and ³J_{C6',H1'}) which are related to the sugar-base torsion angle. These compounds have ³J_{C2',H1'}=1.6-2.2 and ³J_{C6',H1'}=3.7-5.2. Using the Karplus-type curve of Lemieux et al. (Cand. J. Chem. 50 773(1972)) these coupling constants indicate the bases are in an anti-conformation with an average torsion angle of either χ =10 or 110, and that neither the addition of a phosphate to the nucleoside, nor variation of phosphate position (3' or 5') have any measurable effect on the sugar-base torsion angle. Similar studies have been made for 3'- and 5'-AMP. For the study of backbone conformation proton-decoupled spectra were also obtained of 3'-UMP and 5'-UMP at various pH's and ³J_{C2',P} and ³J_{C4',P} were determined to analyse rotation about the C3'-O3' and C5'-O5' bonds. In 5'-UMP, ³J_{C4',P} was found not to be dependent on pH and the *gauche-gauche* rotamer is predominant (~85%). On the other hand, for 3'-UMP ³J_{C2',P} decreased and ³J_{C4',P} increased with increasing pH value. The data indicates a rotamer redistribution of gg(50%), tg(25%) gt(25%) at pH 4.1 to gg(47%), tg(5%) and gt(48%) at pH 8.4, where gg has P *gauche* to both C2' and C4', tg has P *trans* to C2' and *gauche* to C4', and gt has P *gauche* to C2' and *trans* to C4'. These studies are germane to our previously reported studies where ³J_{C2',P} was found to be different in poly A(< 2) and poly U(4.9). (Supported by NSF and NIH.)

W-POS-B9 FAILURE OF PROTEIN SYNTHESIS IN HEAT-KILLED E. COLI. R.G. Dean, E. McGroarty, Dept. of Biophysics, Michigan State University, East Lansing, Michigan 48824

High temperature (48°-70°C) treatment of *Escherichia coli* causes cell death as determined by the inability of the cell to form colonies upon plating. Heating also results in general damage to most systems of the cell. In order to separate more clearly heat damage that causes death from heat damage not causing death, it is necessary to compare heat-killed cells and cells that have been subjected to the same conditions of heating but recover and live. This comparison has been accomplished by separating living from dead cells after heating. *E. coli* CR63 cells were heated until 50% to 70% of the initial population was dead. Subsequent recovery and penicillin treatment lyse the living cells, allowing the dead intact cells to be pelleted by centrifugation. Contamination of the dead cells by living cells or debris is consistently less than 10% of the living population. Contamination of the living fraction by the dead cells may be as high as 30%; however, in this study such contamination is not as important as the contamination of the dead cells by the living population. The protein synthesizing ability of the live vs. dead cell fraction was determined by labeling with leucine C¹⁴ immediately after heating. No uptake of the leucine label, beyond contamination levels, was observed over a period of 90 min. in the dead cell fraction. Live recovering cells, however, showed high levels of leucine incorporation during this same period. This result suggests that some step in protein synthesis or protein stability is crucial in determining if a cell survives or dies. This work supported by funds from NIH Training Grant # GM-01422, and the College of Osteopathic Medicine of Michigan State University.

W-POS-B10 CONFORMATIONAL RELAXATION PROCESSES IN MACROMOLECULES. S.C. Szu and R.L. Jernigan,*
Laboratory of Theoretical Biology, DCBD, National Cancer Institute, National Institute of Health, Bethesda, MD 20014.

Kinetics of helix-coil transitions in both DNA and polypeptides have been treated theoretically. Only two states, helix and random coil, are considered for each molecular unit. The fraction of monomers which is helical is investigated for times following an initial perturbation. Time dependent equations have been developed in a form consistent with the Zimm-Bragg equilibrium scheme. We have not utilized small perturbation theory but have directly calculated the effects of the external perturbation. The large number of conformational states of the system can sometimes be reduced. For short polypeptides it is possible to reduce the states to: 1) the all random coil molecule, 2) molecules containing one unit of helix, and 3) all other forms with more than one helix unit. We have investigated the effects of including a bimolecular reaction for the formation of the first DNA helix unit. The rate of change of the probability of the single strand form depends on a non-integral power of this probability. These non-linear differential equations have been solved numerically. Deviations of these results from those obtained from the polypeptide linear equations are investigated. Available DNA relaxation experiments are compared with our results.

W-POS-B11 CONTROL OF LATE-PROTEIN SYNTHESIS BY BACTERIOPHAGE T4. Elizabeth Kutter, Doug Bradley,* and Linda Breeden,* The Evergreen State College, Olympia, Washington 98505.

The process of T4 morphogenesis has been studied in detail recently, determining the specific roles of some 60 gene products. However, little is known about what controls the relative rates of synthesis of the various proteins. The overall control of late-protein synthesis involves a variety of factors: the extent of DNA production; whether the progeny DNA contains C, HMC, or glucosylated HMC; the properties of the host RNA polymerase; and the polymerase-binding proteins coded for by T4 genes 33,45 and 55. We are using slab gel electrophoresis to examine the relative rates of synthesis when these parameters are varied, in an effort to better understand the controls involved and the nature of the promoters.

We have particularly studied the effects of replacing HMC with C in T4 DNA. Synthesis of all late proteins is greatly inhibited, but some are still produced in significant quantity as long as degradation of the C-containing T4 DNA is prevented (i. e., in a [dCTPase, endonuclease II, endonuclease IV] mutant, which makes DNA at least as large as that made by T4⁺). The relative rates of synthesis of different proteins are very different here than in either a 45⁻ or a DNA⁻ mutant. To better quantitate the effects and the mechanism, we are looking at the effects when C partly replaces HMC, using a ts dCTPase mutant. Surprisingly, all quantifiable late proteins are synthesized at least 30% as fast as with T4D⁺. Electron microscopy showed large numbers of empty heads but no tail structures except polysheath; we are now using sucrose gradients and SDS-urea gels to identify the blocks.

We are also studying the properties of a pseudorevertant, just isolated by Larry Snyder, which allows our [endonuclease II, endonuclease IV, am dCTPase] mutant to produce viable phage in which C largely replaces HMC; we hope to be able to report a great deal more about the nature of the block as a result of these studies.

W-POS-B12 ELECTRON MICROSCOPIC STUDIES OF NUCLEOTIDE SEQUENCE. S.D. Rose,* M.D. Cole,* J.W. Wiggins† and M. Beer, Department of Biophysics, The Johns Hopkins University, Baltimore, Maryland 21218

Cytosine nucleosides and nucleotides readily undergo transamination reactions upon treatment with amines in aqueous bisulfite solution. The use of O-furfurylhydroxylamine results in the quantitative conversion of cytosine nucleosides and nucleotides to N⁴-furfuryloxy derivatives. These derivatives undergo aromatic mercuration at the furan ring. The resulting electron-dense marker is suitable for visualization by electron microscopy. The distribution of markers on nucleic acid molecules is monitored in a high resolution scanning transmission electron microscope assembled at Hopkins. This instrument is capable of showing individual heavy atoms. Thus, its performance appears ample for the study of nucleotide sequence.

W-POS-B13 POSTLABELING OF DNA WITH ^{125}I FOLLOWING SEDIMENTATION IN AN ALKALINE SUCROSE GRADIENT. R.O. Rahn and R.S. Stafford, Biology Division, ORNL, Oak Ridge, TN 37830

Velocity sedimentation in an alkaline sucrose gradient is widely used for analyzing changes in the molecular weight of DNA. To avoid using DNA prelabeled with either ^3H or ^{14}C , we have investigated the feasibility of postlabeling the DNA with ^{125}I . Unlabeled DNA was layered on top of an alkaline sucrose gradient (5-20%) contained in a 4 ml centrifuge tube, sedimented in a swinging bucket rotor and the contents linearly fractionated by dripping into a series of collection tubes. To each fraction was added 13 μg of poly(rA) in order to facilitate complete recovery of the DNA. Following precipitation with 5% TCA and washing with ethanol, the contents of each tube were iodinated in the presence of TiCl_3 according to the method of Commerford (1971).¹ Since cytosine is the only base which is iodinated, the poly(rA) which is present does not interfere in the assay. The reaction mixture without ^{125}I was preincubated at 60°C for 30 min before reaction with DNA in order to reduce background levels below 0.1%. Following incubation at 60°C for 75 min, the reaction was quenched with fresh Na_2SO_3 at pH 9. The contents of each tube (which contained about 10^6 cpm total) were then placed on a filter paper disc, washed with 5% TCA containing 0.01 M KI and rinsed in 95% ethanol. The DNA contained 200-300 cpm/ng and the background counts were on the order of 300-700 cpm per disc. These preliminary results indicate that iodination is a suitable alternative to fluorimetry for analyzing ng amounts of DNA. (Research supported by the U. S. Energy Research and Development Administration under contract with the Union Carbide Corporation.)

¹Commerford, S. L. (1971). *Biochemistry* 10: 1993.

W-POS-B14 RECONSTITUTION OF CHROMATIN SUBUNIT MONOMER PARTICLES, K.G. Tatchell*, K.E. Van Holde, Dept. of Biochemistry and Biophysics, Oregon State University, Corvallis, OR. 97331

Chicken erythrocyte monomer particles containing 140 base pairs of DNA and histones F2a1, F2a2, F2b, and F3 were dissociated in 5 M urea and 2 M NaCl and reconstituted by dialysis into buffers of successively lower ionic strength and urea concentration. The extent and specificity of reconstitution was followed by velocity sedimentation and circular dichroism. 90% reconstitution was obtained as assessed by analytical velocity sedimentation. The reconstituted monomer sedimented as a homogeneous boundary with a sedimentation coefficient of 11S. The reproduction of the characteristic chromatin monomer circular dichroism spectra upon reconstitution suggests high specificity of the DNA-protein interactions. The highest degree of reconstitution was obtained when the urea was dialysed away before the NaCl. This suggests a histone core complex may form as an intermediate in the reconstitution. It is noted that short segments of DNA can reassemble in a specific manner with histone proteins. (Supported by NSF Grant No. BMS 73-06819 A02)

W-POS-B15 INFERENCES FROM CORRECTIONS FOR DIFFERENTIAL LIGHT SCATTERING PRODUCED BY CHROMATIN. F. Kendall, and C. Nicolini, Biophysics Division, Temple University Health Sciences Center, Philadelphia, Pa. 19140

Two methods of correcting for differential light scattering artifacts in the circular dichroism spectra of chromatin are described. The first method utilizes a modification of the J-40 spectropolarimeter to permit the sample cell to be moved progressively as close as possible to the photomultiplier (PM) tube. The monotonically decreasing ellipticity at each sample-PM spacing is extrapolated to zero sample-PM distance where scattered light is treated as transmitted. The second method involves fitting the positive CD (or OD) tail (for any given PM-sample separation) outside the absorptive band ($>310\text{ nm.}$) to a model. The scattering contributions are approximated by extrapolating the fitted curve back through the absorptive band and subtracting the extrapolated values from the observed spectrum. Both methods of correction produce spectra which are in close agreement. Differences in the slope of differential light scattering above 300 nm. have been observed to be associated with chromatin from cells in different functional states. Sheared chromatin produces spectra which are geometry-independent, and which have no positive values at the longer wavelengths outside the absorptive band. These observations suggest that differential light scattering yields new information about the conformation of chromatin in the native condition.

W-POS-B16 DYNAMICS OF CHROMATIN SUBUNITS AND OF WHOLE CHROMATIN. H. Heitzmann, and J. Yguerabide,* Department of Biology, University of California, San Diego. 92093

Independent chromatin subunits, as well as whole chromatin, have been labeled with ethidium bromide; the dynamics of these structures have been investigated by nano-second fluorescence spectroscopy. Subunits ("v-bodies") were prepared from chicken erythrocyte chromatin by nuclease digestion, and purified by sedimentation velocity. The fluorescence anisotropy of labeled v-bodies decayed as a single exponential function, characterized by a rotational correlation time of 100 ± 10 nsec. The data are consistent with a rigid globular particle. The anisotropy decay of ethidium bromide-labeled whole chromatin was also studied, and is analyzed in terms of segmental motion of a chain of subunits.

W-POS-B17 A TRANSITION FROM NON-COOPERATIVE TO COOPERATIVE BINDING OF HISTONE H1 TO DNA ACCOMPANIED BY THE APPEARANCE OF SEQUENCE SELECTIVITY. M. Renz* and L.A. Day. Max-Planck-Institute für Virusforschung, 74 Tübingen (Fed. Rep. of Germany) and The Public Health Research Institute of the City of New York, New York, N.Y. 10016 (U.S.A.)

A sharp transition from non-cooperative to cooperative binding of DNA and histone H1 occurs near 20 mM NaCl in solutions buffered with 5 mM Tris-HCl, pH 7.5. In mixtures containing excess DNA at salt concentrations below this transition concentration, all of the DNA molecules are bound by H1, as shown by their increased sedimentation rate over that of free DNA. At salt concentrations above the transition value, the available histone is distributed in such a way that only part of the DNA is bound by H1 and the rest is free. Below the transition salt concentration, H1 appears not to differentiate between calf lymphocyte DNA and *E. coli* DNA of the same size, but above it the histone shows a strong preference for lymphocyte DNA. In the presence of an excess of calf DNA and under cooperative binding conditions, H1 tends to choose DNA fragments enriched in unique sequences.

W-POS-B18 ION EFFECTS ON PROTEIN--NUCLEIC ACID INTERACTIONS. M. T. Record, Jr., T. M. Lohman and P. L. de Haseth, Department of Chemistry, University of Wisconsin, Madison, Wisconsin 53706

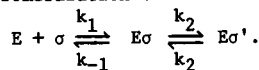
We have developed a general thermodynamic treatment of ion concentration effects on observed association constants (K_{obs}) of protein-nucleic acid interactions. Our approach is based on the linked function analysis of Wyman (Adv. Prot. Chem. 19, 223-286 (1964) and the polyelectrolyte theory of Manning (J. Chem. Phys. 51, 924-933 (1969)), as used previously by us (Biopolymers 14, 2137-2158 (1975)) to treat ion effects on the helix coil transition of DNA. We find that $-(\partial \log K_{obs} / \partial \log Na^+)_{T, pH} = m\psi$ where ψ is the fraction of a counterion thermodynamically bound per phosphate and m is the number of phosphate groups involved in ion-pair formation with the ligand. Once m is known, the electrostatic contributions of ion-pair formation and concomitant counterion release can be determined, and the non-electrostatic component of the binding free energy can be obtained by difference. We have analyzed literature data on the binding of model ligands and the proteins RNase and lac repressor. We have also measured binding constants for the nonspecific interactions of holo and core RNA polymerase with DNA, using quantitative DNA cellulose chromatography. For holoenzyme, $m = 11 \pm 1$ and the binding is purely electrostatic in the nonspecific mode. The lac repressor situation is complex; $m = 14 \pm 2$ in the binding to operator, but we estimate that $m = 7 \pm 2$ in nonspecific binding. The non-electrostatic free energy of operator binding is ~ -6 kcal.

W-POS-B19 A CIRCULAR DICHROISM STUDY OF THE INTERACTION BETWEEN P₃₂ AND DNA. Jan Greve*, Marcos F. Maestre and Junko Hosoda, Space Sciences Laboratory, University of California, Berkeley, California 94720.

The interaction between the DNA unwinding protein P₃₂, isolated from T₄-infected E-coli cells, and DNA has been studied by means of circular dichroism and absorbance spectrometry. In this study we used poly dA-dT and poly dAT-dAT as model compounds for DNA. The spectra of these compounds were measured as a function of temperature, both in the absence and in the presence of the P₃₂ protein. It appeared that the interaction with P₃₂ induces an increase in optical density (260 nm) at temperatures far below the regular melting temperature. The transition between native DNA and the "P₃₂ molten" form takes place over a rather broad temperature interval. The interaction with P₃₂ causes large changes in the circular dichroism spectra of both poly dA-dT and poly dAT-dAT in the wavelength region from 240 to 290 nm. If the differences of the CD spectra in the presence and in the absence of P₃₂ are calculated, it appears that these difference spectra are almost identical for poly dA-dT and poly dAT-dAT. Moreover, the changes in the CD spectra of poly dA-dT and poly dAT-dAT caused by increasing the temperature are similar. From these measurements it is concluded that the structure of the DNA in the DNA-P₃₂ complex at temperatures below the temperature at which complete melting occurs in the absence of P₃₂, is different from a denatured DNA.

W-POS-B20 A CONFORMATIONAL TRANSITION OF E. COLI RNA POLYMERASE INDUCED BY THE INTERACTION OF σ SUBUNIT WITH CORE ENZYME. C.-W. Wu, F.Y.-H. Wu, and L. Yarbrough, Department of Biophysics, Albert Einstein College of Medicine, Bronx, New York 10461.

The isolated σ subunit of RNA polymerase was covalently labeled with a fluorescent probe N-(1-pyrene)maleimide. The labeled σ (PM- σ) retained 80% of its activity in stimulating transcription of T7 DNA by core enzyme as compared to unlabeled σ . The kinetics of the σ -core interaction was investigated with stopped-flow technique monitoring fluorescence quenching of PM- σ by addition of core polymerase. A biphasic change of fluorescence intensity with respect to time was observed when PM- σ was rapidly mixed with core enzyme. The kinetic data can be analyzed in terms of a mechanism in which a bimolecular binding of σ to core enzyme is followed by a relatively slow isomerization of the holoenzyme formed:



The best-fit kinetic parameters are: $k_1 = 3 \times 10^6 \text{ M}^{-1} \text{ sec}^{-1}$, $k_{-1} = 0.23 \text{ sec}^{-1}$, $k_2 = 0.26 \text{ sec}^{-1}$, and $k_2' \leq 1 \times 10^{-3} \text{ sec}^{-1}$. From the parameters, an overall binding constant of $\leq 3 \times 10^{10} \text{ M}$ was estimated for the PM- σ -core complex, in agreement with that obtained by fluorimetric titration. In addition, the following thermodynamic parameters of activation for the conformational transition were obtained by studying the effect of temperature on k_2 : $E^\ddagger = 6.7 \text{ kcal/mol}$, $\Delta G^\ddagger = 18.1 \text{ kcal/mol}$, $\Delta H^\ddagger = 6.1 \text{ kcal/mol}$, and $\Delta S^\ddagger = -40 \text{ entropy units}$. It has been proposed that σ acts on core polymerase to trap a specific conformation of the enzyme which recognizes the proper promoters. In these fluorescent-probe studies we have demonstrated a conformational change of RNA polymerase induced by binding of σ to core enzyme. (Supported by grants NIH GM19062 and Am. Can. Soc. BC-94).

W-POS-B21 QUATERNARY STRUCTURE OF E. COLI RNA POLYMERASE. Z. Hillel and C.-W. Wu, Department of Biophysics, Albert Einstein College of Medicine, Bronx, New York 10461.

E. coli RNA polymerase is a multisubunit enzyme with the composition $\alpha_2\beta\beta'\sigma$. Thus far its complete quaternary structure is not known. We have studied the spatial arrangement of the subunits in core enzyme ($\alpha_2\beta\beta'$) and its stable subcomplex $\alpha_2\beta$ by crosslinking with bifunctional reagents and by fluorescence energy transfer measurements. When core enzyme was incubated with methyl-4-mercaptobutyrimidate-HCl, a cleavable bifunctional reagent, subunit pairs $\beta\beta'$, $\alpha\beta$ and $\alpha\beta'$ were crosslinked as identified by SDS-polyacrylamide gel electrophoresis and confirmed by electrophoresis in the second dimension following cleavage of the crosslinks. In contrast, crosslinking of core enzyme with a longer reagent N,N'-(1,4-phenylene)bismaleimide yielded predominantly two crosslinked bands with molecular weight $\sim 8 \times 10^4$ as calculated from electrophoretic mobility on SDS gels. These bands were interpreted to represent α dimers having different intrapolypeptide crosslinks. Isolated α subunit and $\alpha_2\beta$ subcomplex also produced these two bands upon crosslinking. Based on the above results we conclude that a) the two α subunits in core enzyme and $\alpha_2\beta$ subcomplex are within 12 Å of each other, b) in core enzyme both β and β' subunit are within 7 Å of at least one α subunit, and c) isolated α subunit exists at least in part as dimer. Energy transfer measurements of intersubunit distances carried out with $\alpha_2\beta$ complex reconstituted from a mixture of α subunit randomly surface-labeled with fluorescent donors and α subunit similarly labeled with acceptors indicated that the two α subunits are within contact distance. Further energy transfer and crosslinking studies of both core and holoenzyme are in progress. The distance relationships of the RNA polymerase subunits revealed by these studies will help in understanding the mechanism of promoter recognition and could be used to monitor conformational changes of the enzyme during the process of gene transcription. (Supported by NIH GM-19062 and Am. Canc. Soc. BC-94)

W-POS-B22 LIMITED PROTEOLYSIS OF *E. COLI* INITIATION FACTORS IF-2 AND IF-3.

Sylvia Lee-Huang, Department of Biochemistry, New York University School of Medicine, New York, N.Y. 10016.

Limited trypsinolysis of homogeneous *E. coli* initiation factors IF-2 and IF-3 resulted in specific regions of cleavage.

IF-2 (MW ~94,000) initially yields two fragments: a large fragment (MW ~82,000) which retains IF-2 activity and a small fragment (MW ~12,000) which has no activity. The large fragment can further be cleaved into fragments of 62,000 and 20,000 daltons. The 62,000-dalton fragment retains part of IF-2 activity while the 20,000-dalton species is inactive. Complete loss of activity is concomitant with the scission of the 60,000-dalton fragment to 20,000-dalton fragments.

Under the same conditions, IF-3 (MW ~23,000) is cleaved into two fragments with molecular weights of 14,000 daltons and 9,000 daltons, respectively. Both fragments are inactive in messenger binding, as well as dissociation of 70S ribosomes. Interestingly enough, the 9,000-dalton fragment demonstrated IF-1 activity; it also showed identical electrophoretic mobility on polyacrylamide gel with *E. coli* IF-1 under both native and dissociating conditions.

W-POS-B23 MODEL FOR RUPTURE OF BASE PAIRING IN POLY (A·U) BY FORMALDEHYDE. T.R. Chay, C.L. Stevens, and K-S. Jhung,* Department of Biophysics and Microbiology, University of Pittsburgh, Pittsburgh, Pa. 15260

We have developed a model which describes a rupture process of moderately long poly (A·U) by a slowly reacting agent. This model predicts the following interesting phenomena if the size of polynucleotides is monodisperse: (i) the rate of the rupture is of zeroth order for large portion of the reaction if the denaturation rate is greater than the re-naturation rate; (ii) The rate is of first order for large portion of the reaction if the denaturation rate is about the same as the denaturation rate; (iv) The rupture rate is inversely proportional to the simple power of molecular lengths for Case (i) and to the second power of molecular lengths for Case (ii); (iii) The model gives a precise relation between the ionic strength, temperature, and formaldehyde concentration on the rupture; and (v) The model predicts a critical point at which the reaction switches from the formalization of free U to that of free A. If the size of polynucleotides is polydisperse, then the rate of the rupture becomes first order when the reverse reaction is negligibly small. We have verified these predictions with experiments on poly (A·U).

W-POS-B24 MICROCOCCAL NUCLEASE RESISTANT PORTION OF THE YEAST GENOME. D. Lohr, R. T. Kovacic, and K. E. Van Holde, Department of Biochemistry and Biophysics, Oregon State University, Corvallis, Oregon 97331.

As a beginning toward the goal of physically characterizing the genome of the unicellular eukaryote, baker's yeast, we have studied that portion of yeast chromatin which is resistant *in situ* (intranuclear) to micrococcal nuclease digestion. Previously we have shown that micrococcal nuclease digestion of yeast chromatin produces a series of DNA fragments which are integral multiples of 140 base pair size of DNA ("monomer"). That work has now been extended. (a) The percentage of DNA made acid-soluble and that remaining acid insoluble have been followed as a function of time of digestion. These experiments allow us to estimate the fraction of the genome susceptible to nuclease. (b) Polyacrylamide gel electrophoresis was used to characterize the size of fragments protected from nuclease digestion. Quantitative scanning of the gels yields the amount of monomer (and of multiples of monomer) DNA at various times of digestion. Thus the fraction of the genome involved in being protected in the monomer has been determined. The average size of each of the size classes of fragments was followed accurately as a function of time of digestion by including restriction endonuclease fragments of PM2 DNA in each gel. The size of monomer DNA at long times of digestion corresponds to the nuclease resistant "core" of the monomer; the size of the more susceptible DNA linking the cores can be calculated from the decrease in size of monomer (and multiples) as digestion proceeds.

Supported by NSF Grant BMS 73-06819 A02.

W-POS-B25 EXPERIMENTAL EVIDENCE FOR KINETIC PROOFREADING IN THE AMINOACYLATION OF tRNA^{ile}.
J.J. Hopfield*, Princeton University and Bell Laboratories, and T. Yamane, Bell
Laboratories, Murray Hill, New Jersey, 07974.

Many biochemical reactions are highly specific. In protein synthesis, the point probability of substitution of an incorrect amino acid is less than 10^{-4} . The paradigm for discrimination is Michaelis kinetics, where an enzyme *b* which recognizes and acts on substrate *B* but reacts less well with incorrect *C*. The rate of making errors is related to the maximum difference ΔG in the free energies for the two reactions along the reaction path, and the error fraction is $f_0 \approx \exp(-\Delta G/KT)$. Kinetic proofreading¹⁾ is a reaction scheme of a more complicated topology, with a necessary energy coupling and a high energy intermediate, which leads to a proofreading for errors (even without leaving the recognition site) and an error rate f_0^2 for a given ΔG . We have measured the charging of tRNA^{ile} with the enzyme isoleucyl synthetase for the correct amino acid (isoleucine) and for incorrect valine. In this system, the proofreading decrease in error rate can be determined by measuring the stoichiometry between ATP hydrolysis and the aminoacylation of tRNA. For ile, we find 1.4 ATP hydrolyzed per tRNA charged, but for val, 220. The experimental key to the measurements is the prevention of the hydrolysis of charged tRNA. In the kinetic scheme of tRNA^{ile} charging, this demonstrates a kinetic proofreading-induced reduction in errors by a factor of 1.4/220. The initial Michaelis complex is known to discriminate between val and ile at a level of about 1/100. Thus we can understand a net error rate of less than 10^{-4} as due to the use of kinetic proofreading on a fundamental error rate of 1/100.

*Work at Princeton supported in part by NSF grant DMR 75-14264

¹⁾J.J. Hopfield, *Proc. Nat. Acad. Sci.* 71, 4135 (1974)